On the Physical Carrier Sense in Wireless Ad Hoc Networks

Xue Yang and Nitin H. Vaidya
Department of Electrical and Computer Engineering, and
Coordinated Science Laboratory
University of Illinois at Urbana-Champaign
email: xueyang, nhv@uiuc.edu

Technical Report, July 2004

***Abstract*— The aggregate throughput of a wireless ad hoc network depends on the channel capacity, channel utilization (i.e., the fraction of channel capacity used for generating goodput), and the concurrent transmissions allowed in the network. While channel utilization is determined by MAC overhead, physical carrier sense has been used as an effective way to avoid interference and exploit spatial reuse. Prior research has attempted to identify the optimal carrier sense range that can maximize the aggregate throughput. However, the impact of MAC overhead has been ignored. In this paper, we use both an analytical model and simulation results to show that MAC overhead has significant impact on the choice of optimal carrier sense range. If MAC overhead is not taken into account properly in determining the optimal carrier sense range, the aggregate throughput can suffer a significant loss.**

***Index Terms*— System design, Simulations, Wireless ad hoc networks, Physical carrier sense, MAC overhead, Spatial reuse**

I. Introduction

Two fundamental aspects of wireless communication make wireless networks different from wired networks. First is the time-variation of the channel strengths due to the small-scale effect of multipath fading, as well as larger scale effects such as path loss via distance attenuation and shadowing by obstacles. Second, wireless stations communicate over the air and there is significant interference among stations that are spatially close to each other.

Whether two wireless stations can communicate with each other depends on the distance between them, the terrain, the transmission power used by the transmitter, etc. Additionally, the quality of the communication link depends on the interference at the receiver caused by other concurrent transmissions in the network (by concurrent transmissions, we mean the transmissions that overlap in time.). The higher the Signal-to-Interference-and-Noise-Ratio ($SINR$), the higher rate can packets be transmitted reliably. As a result, the channel capacity between a transmitter/receiver pair is a function of channel activities of all stations in the network. On the other hand, because of the rapid attenuation of transmitted radio signal with distance, concurrent transmissions that reuse the same channel at spatially separated locations are possible, which leads to co-channel spatial reuse in wireless networks. The aggregate throughput of a network depends on both the capacity of each individual link and the total amount of concurrent transmissions allowed in the network.

Furthermore, medium access control (MAC) protocols play an important role in utilizing the link capacity. In ad hoc networks, which are formed by a group of self-organizing wireless stations without the support of access points, stations typically contend for access to the channel in a distributed fashion. Among multiple stations that contend the channel with each other, when only one makes a transmission attempt, the packet is delivered successfully; if multiple contending stations make transmission attempts simultaneously, collisions may occur. Stations resolve the channel contention according to rules defined by the contention resolution algorithm. MAC protocols often introduce overhead that leads to a sub-optimal utilization of the link capacity.

MAC protocols also govern when concurrent transmissions may proceed. One representative method is based on CSMA (carrier sense multiple access). Carrier sense refers to listening to the physical medium to detect any ongoing transmissions. Only if the radio signal strength detected at a station is below a *Carrier Sense Threshold*, may the attempt of the station to access the channel proceed. Given a carrier sense threshold CS_{th}, the corresponding *Carrier Sense Range* D is defined as the minimum distance allowed between two concurrent transmitters.

Prior research has noted the impact of carrier sense range on the aggregate throughput. That is, the smaller

This work is supported in part by the National Science Foundation Grant ANI-0125859 and Vodafone Graduate Fellowship.

the carrier sense range, the better the spatial reuse; but the interference at a receiver can also increase. Implicitly assuming a *perfect* MAC protocol without any overhead, Zhu *et al.* [1] has attempted to identify the optimal carrier sense threshold that maximizes the spatial reuse given a minimum required $SINR$ for a regular topology. However, the interactions between carrier sense range and MAC overhead, as well as their impact on the network aggregate throughput, have not been identified by prior research. In this paper, we use both an analytical model and simulation results to show that the MAC overhead has a significant impact on the choice of the optimal carrier sense range that maximizes the aggregate throughput. If MAC overhead is not taken into account properly in determining the optimal carrier sense range, the aggregate throughput can suffer a significant loss.

The rest of the paper organized as follows. Section II summarizes the related work. Section III introduces bandwidth-independent and bandwidth-dependent MAC overhead. In Section IV, a analytical model is presented to explore the impact of MAC overhead on the optimal carrier sense range, and associated impact on the aggregate throughput. Section V uses simulation results to further support our arguments. Finally, conclusions and future work are presented in Section VI.

II. Related Work

While MAC protocols govern when a station may proceed its transmission attempt, the channel access activities of all stations in the network contribute to the aggregate interference at a particular receiver, which, in turn, determines the performance of MAC protocols. The inherent interactions between MAC and physical (PHY) layer necessitate considering the MAC and PHY characteristics together. However, many prior research works have treated MAC and PHY layer characteristics separately when discussing the design issues for wireless ad hoc networks. For example, to combat the hidden terminal problem in ad hoc networks, the earlier work [2] has proposed to use RTS/CTS handshake method, in which RTS (Request To Send) and CTS (Clear To Send) frames are exchanged to reserve the channel for subsequent Data and ACK packets. Stations that overhear the RTS/CTS frames defer transmission for a certain period. This method is adopted by IEEE 802.11 DCF [3], and named as "virtual carrier sense". RTS/CTS handshake works if all stations that may cause interference at a receiver are within the transmission range of the receiver. However, after considering the physical characteristics of radio signal propagation carefully, it can be shown that many interfering stations can actually locate outside the transmission range of the receiver. Therefore, RTS/CTS method may not work properly in ad hoc networks, as has been discussed in detail in [4].

Physical carrier sense can help to avoid the interference at a receiver effectively as long as the potential interfering stations are able to sense the radio signal from the transmitter. Physical carrier sense can also help to control the amount of spatial reuse in the network by varying the carrier sense threshold. Zhu *et al.* [1] has attempted to identify the optimal carrier sense threshold that maximizes the spatial reuse given a minimum required $SINR$ for a regular topology. The limitation of their work lies in that they do not consider the MAC overhead as well as the interactions between MAC overhead and the carrier sense range.

To derive the capacity of wireless networks, Gupta and Kumar [5] incorporate the physical channel model wherein a minimum $SINR$ is necessary for successful communication. [6] proposes a Honey-grid model to calculate the interference level in wireless ad hoc networks. The derived expected values of $SINR$ are used to determine the network capacity and data throughput per node. [7] presents an analytical model to investigate co-channel spatial reuse in dense wireless ad hoc networks based on RF propagation models. A common limitation of above works is that they all assume a perfect MAC protocol with no overhead, which is not practically achievable.

In this paper, we are interested in exploring the interactions between MAC and PHY layers, identifying the impact of MAC overhead on the choice of optimal carrier sense range, as well as the associated impact on the aggregate throughput.

Some research work does consider the impact of physical layer on MAC layer more explicitly, with a different objective from this paper. For example, Holland *et al.* [8] propose a receiver-based rate-adaptive MAC protocol, in which the link rate between the transmitter/receiver pair is dynamically chosen based on the $SINR$ level at the receiver. Considering the quality variation of wireless links, Sadeghi *et al.* [9] proposes an opportunistic MAC protocol which sends multiple back-to-back data packets whenever the channel quality is good to better exploit durations of high-quality channel conditions. [10] proposes an enhanced carrier sensing (ECS) scheme to modify the EIFS based deferment in IEEE 802.11 DCF such that the EIFS duration depends on the type of the erroneous frame (CTS, Data or ACK). [11] constructs a collision model and an interference model to identify the optimal transmission power that can yield the maximum throughput and the minimum energy consumption per message. [12] introduces a modeling framework for the analytical study of MAC protocols operating in ad hoc

networks. The model explicitly takes into account the effect of physical-layer parameters on the success of transmissions.

III. Bandwidth-independent and Bandwidth-dependent MAC overhead

MAC overhead can be generally categorized into *bandwidth-independent overhead* and *bandwidth-dependent overhead*, as pointed out in [13]. Specifically, if the channel time consumed by an overhead is independent of the channel bit rate, the overhead is defined as bandwidth-independent overhead; otherwise, it is bandwidth-dependent overhead[1].

Consider one of the standards for wireless networks, IEEE 802.11 WLAN [3], as an example. Different physical layer specifications are defined in IEEE 802.11. Direct sequence spread spectrum (DSSS) system (802.11b) provides 1 Mbps, 2 Mbps, 5.5 Mbps and 11 Mbps data transmission rates, operating in the 2.4 GHz ISM band [14]. To allow the IEEE 802.11 MAC to operate with minimum dependence on the physical layer, a physical layer convergence procedure (PLCP) is defined. PLCP preamble and header aid receivers in demodulation and delivery of transmitted data units from MAC layer. For each data unit transmitted by MAC layer, 192 μs additional channel time is consumed by PLCP preamble and header. Orthogonal frequency division multiplexing (OFDM) system (802.11a) operating in the 5 GHz band provides data payload communication rates from 6 Mbps to 54 Mbps [15], with PLCP preamble and header overhead of 20 μs associated with each MAC layer data unit transmitted. For both DSSS and OFDM systems, the channel time consumed by PLCP preamble and header is independent of the channel bit rate, resulting in bandwidth-independent overhead.

In one of the MAC layer sub-functions, IEEE 802.11 DCF (Distributed Coordinated Function), a station wanting to access the channel has to wait the channel to be idle for an "interframe space (IFS)" duration. After that, a backoff procedure is invoked and a backoff counter is randomly chosen from the range of [0, CW] (CW represents the contention window). This backoff counter corresponds to the number of idle slots this station has to wait before its transmission attempt. Since the slot time is determined by the propagation delay and the transceiver's turnaround time[2], the interframe space and the backoff durations are independent of the channel bit rate, hence, they also contribute to the bandwidth-independent overhead.

A packet transmission can be corrupted by the interference at a receiver. In wireless networks, a station usually can only learn about a transmission failure when the transmission is finished and the expected acknowledgment (in some form) does not come back. Consequently, a transmission failure will result in the loss of entire packet transmission duration, which depends on the packet size and the channel bit rate. Therefore, the overhead associated with transmission failures is bandwidth-dependent overhead.

One key property of bandwidth-independent overhead is that, the larger the channel bit rate, the more the percentage of wasted channel capacity. Let T (in seconds) represent the duration of channel time occupied by the bandwidth-independent overhead, R be the channel bit rate (in bits per second or bps) and P_l be the payload size (in bits) associated with the overhead. Accordingly, $\frac{TR}{P_l}$ fraction of the channel capacity is wasted in the bandwidth-independent overhead. Clearly, the smaller the R, the less the channel wastage.

Alternatively, given a modulation scheme, channel bit rate is proportional to the channel bandwidth. For a given packet size, the bandwidth-independent overhead can be reduced by associating it with a channel with a smaller bandwidth. That is, by splitting a channel into multiple sub-channels, the utilization of each sub-channel may get improved due to the reduced channel wastage in the bandwidth-independent overhead, which can lead to an improved aggregate throughput over all sub-channels, comparing with using a single channel. An earlier paper [16] implicitly applied such an idea to mutli-channel wired networks.

In wireless ad hoc networks, motivated by this observation, we can let a wireless link operate at a lower bit rate to improve the utilization of the single channel. Here, channel utilization is defined as the fraction of channel capacity used for generating goodput. At the same time, since a lower bit rate usually requires less $SINR$, more interference can be tolerated at the receiver given the signal strength of the intended signal. As a result, more concurrent transmissions can proceed and more spatial reuse can be exploited. The aggregate throughput can be improved due to the following two reasons:

- Despite operating at a lower rate, each wireless link can be utilized more efficiently because a smaller fraction of channel capacity is wasted in MAC overhead.
- More concurrent transmissions are allowed in the

[1]We follow the terms used in [13] here. However, it is probably more accurate to name them as rate-independent and rate-dependent overhead under the context we consider in this paper.

[2]The turnaround time is the delay associated with the transceiver in switching between transmitting and receiving modes.

network. As illustrated in Figure 1, three concurrent transmissions are allowed in scenario (b), while only two are allowed in scenario (a). The increased aggregate throughput can result from more concurrent transmissions, even though the absolute rate of each individual link is lower.

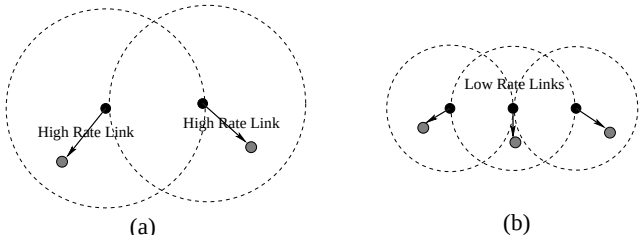

Fig. 1. More concurrent transmissions

By extending above concepts to MAC protocols using physical carrier sense, we show in the rest of this paper that, not only the bandwidth-independent overhead but also the bandwidth-dependent overhead can be reduced by applying a smaller carrier sense range, which, in turn, affects the choice of optimal carrier sense range for wireless ad hoc networks.

IV. Optimal Carrier Sense Range

In this section, we develop an analytical model to derive the optimal carrier sense range with and without considering MAC overhead. In the model, a dense network is assumed and wireless stations are uniformly and independently distributed in an area of A. A common and fixed transmission power P is used by each transmitter. The minimum received signal strength that invokes the packet receiving procedure at a receiver is defined as *Receiving Signal Threshold*, denoted as RX_{th}. Given the value of RX_{th}, the *Maximum Transmission Range* R, which is defined as the maximum possible distance between the transmitter and receiver, can be determined accordingly based on the radio propagation model. The link capacity between the transmitter/receiver pair depends on $SINR$ at the receiver.

Two concurrent transmissions may occur if and only if the distance between the two transmitters is larger than the carrier sense range D. The larger the carrier sense range, the less the interference and the better the $SINR$ at the receiver. Consequently, the wireless link between the transmitter/receiver pair can operate at a higher rate. On the other hand, a large carrier sense range may severely limit the aggregate throughput since each station becomes too conservative in initiating a transmission and the number of concurrent transmissions decreases. Such a tradeoff implies that there exists an optimal carrier sense range that maximizes the aggregate throughput.

A. Interference Model

We first derive the worst case interference and $SINR$ at a receiver station. The radio propagation model used in this paper is given by:

$$P_{rx} = \frac{P}{r^{\theta}}$$

where P_{rx} is the received signal strength given the transmission power P, r is the distance between the transmitter and receiver, and θ is the path loss coefficient, ranging from 2 (free space) to 4 (indoor) [17].

As shown in Figure 2(a), when a source station S_0 is transmitting, a concurrent transmission can happen only at a station, say S_1, that is distance D away from station S_0, constrained by the carrier sense range of D. Moreover, when stations S_0 and S_1 are transmitting at the same time, the next concurrent transmission can only come from stations that are distance D away from both S_0 and S_1, say S_2. Defining the concurrent transmitting stations that are iD (where i is an integer and $i \geq 1$) distance away from S_0 as the i^{th} tier interfering stations for S_0, there are at most six 1^{st} tier interfering stations, as illustrated in Figure 2(a).

The spatial reuse in ad hoc networks is very similar to that in cellular networks. In the cellular system, *co-channel cells* in a given coverage area can reuse the same set of frequencies. To reduce the co-channel interference, co-channel cells must be physically separated by a minimum distance to provide sufficient isolation [18].

Among the six 1^{st} tier interfering stations, it has been shown in [19] in the context of cell planning in cellular networks that, with a receiving station, R_0, at the edge of the transmission range, the worst case interference comes from the two nearest interfering stations that are $D - R$ away from the receiving station, and four other interfering stations that are exactly $D-R/2$, D, $D+R/2$, $D + R$, respectively, away from the receiving station, as illustrated in Figure 2(b).

Both [20] and [21] have observed the fact that the received power at a receiver station from the nearest neighbor is of the same order as the total interference from the entire network. As the interference from the 1^{st} tier interfering stations dominates, we neglect the remaining interference from the 2^{nd} tier or further away interfering stations. As such, the worst case interference at the receiving station R_0 can be expressed as below.

$$Interference = \frac{2P}{(D-R)^{\theta}} + \frac{P}{(D-\frac{R}{2})^{\theta}} + \frac{P}{D^{\theta}} + \frac{P}{(D+\frac{R}{2})^{\theta}} + \frac{P}{(D+R)^{\theta}}$$

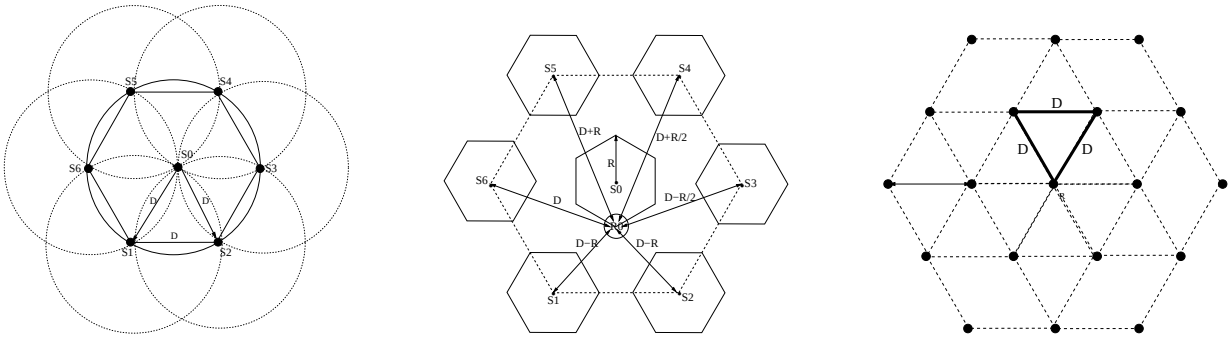

(a) Nearest concurrent transmissions

(b) The first tier interfering stations

(c) Multiple concurrent transmissions

Fig. 2. Interference model

As the receiving station R_0 (in Figure 2(b)) is positioned at the edge of the transmission range (i.e., R distance away from the transmitter S_0), it has the weakest receiving signal strength (within S_0's transmission range). The corresponding worst case $SINR$ at the receiving station R_0 is shown below, where $X = \frac{D}{R}$ (note that the background noise is ignored here since we mainly concern an interference limited environment).

$$\begin{aligned} SINR &= \frac{\frac{P}{R^\theta}}{\frac{2P}{(D-R)^\theta} + \frac{P}{(D-\frac{R}{2})^\theta} + \frac{P}{D^\theta} + \frac{P}{(D+\frac{R}{2})^\theta} + \frac{P}{(D+R)^\theta}} \\ &= \frac{1}{\frac{2}{(X-1)^\theta} + \frac{1}{(X-\frac{1}{2})^\theta} + \frac{1}{X^\theta} + \frac{1}{(X+\frac{1}{2})^\theta} + \frac{1}{(X+1)^\theta}} \end{aligned} \quad (1)$$

B. Optimal Carrier Sense Range without MAC Overhead

Given a certain $SINR$, we use *Shannon capacity* as the achievable channel rate, i.e.,

$$ChannelRate = W \log_2 (1 + SINR)$$

where W is the channel bandwidth in hertz and an additive white Gaussian noise channel is assumed [22].

Since the minimum separating distance between two concurrent transmissions is D, each transmitter "consumes" a certain area A_s. On one extreme, when there is only one transmitter in the network, it is straightforward to see that $A_s = 3\sqrt{3} * D^2/2$. On the other extreme, with an infinite number of concurrent transmitters, a triangle area, as highlighted in Figure 2(c), is shared by 3 concurrent transmitters and each transmitter shares six such triangles. Consequently, we have $A_s = \sqrt{3}D^2/2$. In a network with an arbitrary number of concurrent transmitters, A_s is proportional to D^2 and we represent A_s as $A_s = C_0 * D^2$, where C_0 is a constant depending on the size of the network ($\sqrt{3}/2 \leq C_0 \leq 3\sqrt{3}/2$).

As we are interested in the maximum achievable aggregate throughput, a busy network is assumed in which each station is always backlogged and it will initiate a transmission whenever it is allowed. With a perfect MAC scheduling algorithm without any overhead, each communication link can be fully utilized and the network aggregate throughput denoted as $Thrput$ can be represented as:

$$\begin{aligned} Thrput &= ChannelRate * \frac{A}{A_s} \\ &= C_1 * \frac{\ln (1 + SINR)}{X^2} \end{aligned} \quad (2)$$

where $\frac{A}{A_s}$ accounts for the total number of concurrent transmissions (ignoring edge effect), and C_1 is a constant defined as $C_1 = \frac{W*A}{C_0 * \ln 2 * R^2}$.

Substituting Equation 1 into Equation 2, we can then identify how the aggregate throughput changes with the value of carrier sense range. When $SINR$ is very small, $\ln (1 + SINR)$ increases nearly linearly with $SINR$, which, in turn, increases fast with X. A larger X leads to a higher throughput. On the other hand, when $SINR$ is very large, the logarithmic increase of $\ln (1 + SINR)$ with respect to $SINR$ implies that the throughput will begin to decrease with the further increase of X. Based on Equation 2, the optimal values of X that maximize the aggregate throughput are solved for various values of θ, and are plotted in Figure 3. X axis represents the path loss coefficient θ, while y axis represents the optimal X corresponding to each θ. The results suggest that, without considering the MAC overhead, the optimal carrier sense range D should be 3.3 times the maximum transmission

range R when $\theta = 4$, be 3.2 times R when $\theta = 3$, and be 2.7 times R when $\theta = 2$.

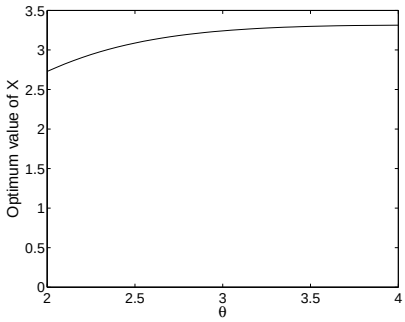

Fig. 3. Optimal X without MAC overhead

C. Optimal Carrier Sense Range with MAC Overhead

Now we consider the impact of MAC overhead on the values of optimal carrier sense range. Let c represent the packet pay load size (in bits). To schedule a successful packet transmission, the associated bandwidth-dependent overhead, denoted by b (bits), and the bandwidth-independent overhead, denoted by a (seconds), are introduced by MAC layer.

The aggregate throughput can thus be represented as:

$$Thrput = \frac{c}{a + \frac{b+c}{Channel\,Rate}} * \frac{A}{A_s}$$

where $\frac{c}{a+\frac{b+c}{Channel\,Rate}}$ is the actual throughput obtained by each transmitter/receiver pair and $\frac{A}{A_s}$ reflects the total number of concurrent transmissions. Simplifying the above equation, we have

$$Thrput = C_1 * \frac{c}{b+c} * \frac{1}{(\frac{aW}{(b+c)\ln 2} + \frac{1}{\ln(1+SINR)})X^2} \quad (3)$$

C_1 is the same constant item defined in Equation 2. Notice that when $a = 0$ and $b = 0$, Equation 3 reduces to Equation 2.

Let O_i denote the term $\frac{aW}{(b+c)\ln 2}$ in Equation 3. The unit of O_i is hertz/bps. We can see that O_i reflects the ratio of the wasted channel spectrum in bandwidth-independent overhead over the sum of the bandwidth-dependent overhead and the payload.

1) With Bandwidth-independent Overhead Only ($a > 0$, $b = 0$): The first sub-case we consider is that there is only bandwidth-independent MAC overhead.

As we discussed in Section III, when multiple stations compete for a *common* channel, the smaller the channel bit rate, the smaller fraction of channel capacity is wasted in associated bandwidth-independent overhead and the better the channel utilization. At the same time, since a lower bit rate typically requires less $SINR$, more interference can be tolerated and more concurrent transmissions are allowed. Even though each communication link operates at a lower bit rate, the aggregate throughput may be improved due to a better channel utilization and the improved spatial reuse. Therefore, we expect the optimal carrier sense range with bandwidth-independent overhead to be smaller compared with the case where no MAC overhead is considered.

The same conclusion can be reached by observing Equation 3. With $a > 0$ and $b = 0$, we have a non-zero O_i. Comparing Equations 3 and 2, because the item $\frac{1}{(O_i + \frac{1}{\ln(1+SINR)})}$ increases slower than $\ln(1 + SINR)$ with the increase of X, the optimal value of X resulting from Equation 3 is smaller than that obtained from Equation 2.

Based on Equation 3, the optimal values of X that maximize the aggregate throughput are obtained for the cases of $O_i = 0.2, 0.5, 1$ hertz/bps, and are plotted in Figure 4. The curve with no MAC overhead (i.e., $O_i = 0$) from Figure 3 is also shown here for the purpose of comparison. To have a sense for what could be the practical values for O_i, we can do some simple calculations here for IEEE 802.11a. In 802.11a, the PLCP preamble and header consume 20 μs for each transmitted data packet, and the SIFS is 16 μs. The bandwidth occupied by each channel is 16.6 MHz (i.e., W = 16.6 MHz); the slot time is 9 μs. Assuming the payload size c is 512 bytes, then $O_i = 0.21$ when there is no backoff slot, and $O_i = 0.63$ with eight backoff slots. 802.11b can have larger O_i because of a longer PLCP preamble and header, as well as a longer slot time.

From Figure 4, we can see that, with the increase of O_i, the optimal value of X decreases for various values of θ. Particularly, when $\theta = 4$, the optimal X is 3.3, 2.9, 2.6, 2.4 for O_i = 0, 0.2, 0.5, 1 hertz/bps, respectively.

2) With both Bandwidth-independent and Bandwidth-dependent Overhead ($a > 0$, $b > 0$): Now we further consider the sub-case in which both the bandwidth-independent and bandwidth-dependent MAC overhead exist. From now on, we strictly differentiate the term concurrent transmissions from the term simultaneous transmissions. Concurrent transmissions refer to trans-

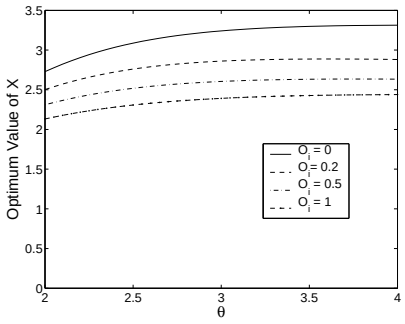

Fig. 4. Optimal X with bandwidth-independent overhead

missions that overlap in time, while simultaneous transmissions refer to the transmissions that start within a short period (i.e., the propagation delay and carrier sense delay) before the carrier can be detected.

For a receiver, there are mainly two sources of interference. One interference source is the concurrent transmissions from transmitters outside the carrier sense range. As illustrated in Figure 5, with a carrier sense range of D, the stations that are outside the outer circle are allowed to transmit at the same time when S0 is transmitting, which causes interference at S0's receiver. The other interference source results from what we usually refer to as *collisions*, when the simultaneous transmission attempts from transmitters inside the carrier sense range occur. For example, in Figure 5, if S0 *has already begun* its transmission, the stations that are inside the carrier sense range D can sense the busy channel and defer their transmissions; but if they start their transmissions simultaneously with S0, S0's transmission will be interfered by them.

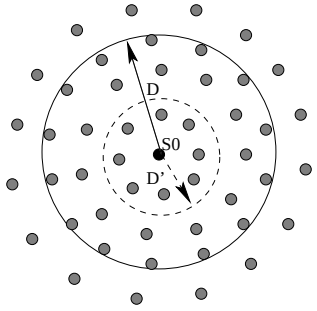

Fig. 5. The impact of carrier sense range on bandwidth-dependent overhead

When reducing the carrier sense range, the increased interference from concurrent transmissions is taken into account when we estimate $SINR$ at the receiver and choose a communication link rate accordingly; but the interference from simultaneous transmitters inside the carrier sense range has not been taken into account. In many MAC protocols (e.g., IEEE 802.11 DCF), the probability of simultaneous transmissions (i.e., collision probability) increases with the total number of contending stations. As illustrated in Figure 5, when reducing the carrier sense range from D to D', the number of contending stations inside the carrier sense range reduces, which leads to the reduced collision probability with S0, thus, less retransmissions and less bandwidth-dependent overhead (recall that interference from concurrent transmitters outside the carrier sense range is accounted for when choosing the bit rate). The reduced bandwidth-dependent overhead at a smaller carrier sense range can further affect the choice of optimal carrier sense range, making it even smaller compared with the cases that do not consider the bandwidth-dependent overhead.

As the probability of collision varies with different MAC protocols, a MAC protocol needs to be specified in order to have numerical comparisons. In the following, we assume a p-persistent MAC protocol, in which, at each time slot, a station chooses to transmit with probability p[3].

In Equation 3, the bandwidth-dependent overhead b depends on the collision probability, which, in turn, depends on the choice of X. Given M contending stations, the average number of collisions per transmission cycle, denoted as $E[N_c]$, is derived in [23] as follows.

$$E[N_c] = \frac{1-(1-p)^M}{Mp(1-p)^(M-1)} - 1. \quad (4)$$

Assuming that there are k stations per transmission area πR^2 (i.e., the area covered by the maximum transmission range R), the number of contending stations M given the carrier sense range D can be represented as

$$M = k\frac{\pi D^2}{\pi R^2} = kX^2 \quad (5)$$

Recall that c represents the payload size. As each collision lasts for the payload transmission duration (we ignore propagation delay and carrier sense delay here for simplicity), we have

$$b + c = E[N_c] * c + c = (E[N_c] + 1) * c \quad (6)$$

Let a_{inv} be the bandwidth-independent overhead associated with each transmission attempt. The total bandwidth-independent overhead a can thus be represented as $a = (E[N_c]+1)a_{inv}$, and O_i can be represented as $O_i = \frac{aW}{(b+c)\ln 2} = \frac{a_{inv}W}{c\ln 2}$. O_i can be regarded as a fixed value when varying b if a_{inv} changes little with b, which is the case we consider here.

[3][23] shows that IEEE 802.11 DCF can be nicely modeled as a p-persistent protocol.

By substituting Equations 4, 5, and 6 into Equation 3, letting $p = 0.02$ and O_i = 0.5 hertz/bps, the optimal X that maximizes the aggregate throughput for the cases of $k = 5$ and $k = 20$ are plotted in Figure 6, along with the two curves from Figure 4 with $O_i = 0$ and $O_i = 0.5$, where no bandwidth-dependent overhead is considered.

As we can see, the optimal X decreases with the increase of channel contention (when k is increased from 5 to 20). Particularly, when $\theta = 4$, the optimal X is 2.4 for $k = 5$ and 2.1 for $k = 20$. When compared with the optimal X = 3.3 when $O_i = 0, b = 0$, and the optimal X = 2.6 when $O_i = 0.5, b = 0$, we can also observe that the optimal X is even smaller when bandwidth-dependent overhead is taken into account.

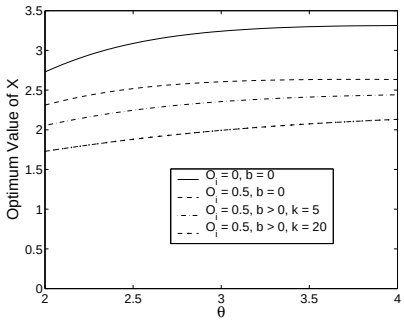

Fig. 6. Optimal X with bandwidth-independent and bandwidth-dependent overhead

D. Impact on Aggregate Throughput

Above discussions suggest that the overhead introduced by MAC layer leads to a smaller choice for the optimal carrier sense range. The carrier sense range is a concept introduced for ease of understanding. In practical systems, a wireless transceiver determines the channel status based on the carrier sense threshold CS_{th} and it does not know the carrier sense range itself. Therefore, from now on, our discussions will be based on carrier sense threshold instead of carrier sense range. Notice that a *larger* carrier sense threshold leads to a *smaller* carrier sense range.

Given $CS_{th} = \frac{P}{D^\theta}$ and $RX_{th} = \frac{P}{R^\theta}$, we have $\frac{CS_{th}}{RX_{th}} = (\frac{1}{X})^\theta$. Defining $\beta = \frac{CS_{th}}{RX_{th}}$, Equation 3 can be rewritten as

$$Thrput = C_1 * \frac{c}{b+c} * \frac{1}{O_i + \frac{1}{\ln(1+SINR)}} * \beta^{\frac{2}{\theta}} \quad (7)$$

For the cases of $O_i = 0$ and $b = 0$ (no MAC overhead), $O_i = 0.5$ and $b = 0$ (with bandwidth-independent overhead only), $O_i = 0.5$ and $k = 5$, as well as $O_i = 0.5$ and $k = 20$ (with both bandwidth-dependent and bandwidth-independent overhead but different transmitter densities), we plot the aggregate throughput $Thrput$ vs. β in Figure 7, assuming $\theta = 4$ and $p = 0.02$. The obtained throughput is normalized to the maximum value in the plot.

From Figure 7, we can see that, if carrier sense threshold is not adjusted according to the MAC overhead, the aggregate throughput suffers. Particularly, when applying the optimal carrier sense threshold with no MAC overhead to the case $O_i = 0.5$ and $b = 0$, the aggregate throughput degrades about 15% compared with the achievable peak throughput; when it is applied to the case $O_i = 0.5$ and $k = 5$, the aggregate throughput degrades as much as 49% compared with the achievable peak throughput; the aggregate throughput suffers even more when it is applied to the case $O_i = 0.5$ and $k = 20$.

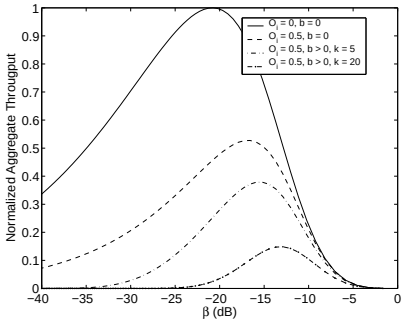

Fig. 7. Aggregate throughput with bandwidth-independent and bandwidth-dependent overhead

V. Discrete Multi-rate Wireless Network

Some assumptions used by the analysis in Section IV may not be feasible in real systems. For example, a very dense network has been assumed such that a source station is always available at any desired place to exploit the potential spatial reuse. In real networks, source stations are usually separated by a certain distance. Additionally, by applying Shannon capacity formula, the link rate is a continuous function of $SINR$ at the receiver. But, typically, a wireless transceiver in practical use only provides multiple discrete rate levels. Each link rate has a minimum required $SINR$ (i.e., $SINR$ threshold). The higher the rate, the higher the corresponding $SINR$ threshold.

In this section, we use simulations to further study the validity of our arguments in discrete multi-rate wireless networks. The simulations are performed using ns-2 simulator version 2.26. In this version of ns-2, each individual interfering signal picked up by a receiver is treated separately to determine whether it will interrupt

Rates (Mbps)	$SINR$ (dB)	Modulation	Coding Rate
54	24.56	64-QAM	3/4
48	24.05	64-QAM	2/3
36	18.80	16-QAM	3/4
24	17.04	16-QAM	1/2
18	10.79	QPSK	3/4
12	9.03	QPSK	1/2
9	7.78	BPSK	3/4
6	6.02	BPSK	1/2

TABLE I

FOR BERS LESS THAN OR EQUAL TO 1E-5, THE MINIMUM REQUIRED $SINR$ CORRESPONDING TO EACH DATA RATE

the receiver's current reception or not. However, even though a single interfering signal may not strong enough to interfere, collectively, the aggregate interference from many concurrent transmissions might do. Therefore, we made the necessary modifications to the related modules of ns-2 so that the interference from all concurrent/simultaneous transmissions will be accumulated to calculate the $SINR$ at a receiver. Two-ray ground radio propagation model is used in the simulations.

The physical layer characteristics used in the simulations follow the specifications of IEEE 802.11a, where the $SINR$ threshold required for each data rate is listed in Table I [24]. Notice that the same modulation scheme (64-QAM) is applied to both data rates of 54 Mbps and 48 Mbps. The different data rates only result from different coding rates, which explains why the $SINR$ thresholds of 54 Mbps and 48 Mbps are very close. Due to their close $SINR$ thresholds, the data rates of 54 Mbps and 48 Mbps show similar performance trends for the issues we are interested in. Thus, we only present the results of 54 Mbps for clarity. Similarly, we present the results of 36 Mbps from the pair of 36 and 24 Mbps, 18 Mbps from the pair of 18 and 12 Mbps, 9 Mbps from the pair of 9 and 6 Mbps.

The MAC protocol used follows the specifications of IEEE 802.11 DCF. As we are interested in the maximum achievable aggregate throughput, Constant Bit Rate (CBR) traffic is used and the traffic sending rate is aggressively enough to keep each source station constantly backlogged. The simulated topology is a symmetric circular topology, in which N transmitters are evenly distributed along a circle with a radius of 350 meters. The receiver corresponding to a transmitter locates on the line from the transmitter to the center of the circle, and is 35 meter away from the transmitter. One example of the simulated topology with N = 8 (i.e., eight transmitters) is shown in Figure 8. The chosen signal receiving threshold RX_{th} corresponds to the maximum transmission range R = 35 meters. Note that symmetric topologies help us to illustrate the issues discussed earlier. Also, in a symmetric topology, it is appropriate to use identical carrier sense threshold at all stations. In arbitrary topologies, each station may have its own optimal carrier sense threshold depending on its neighborhood.

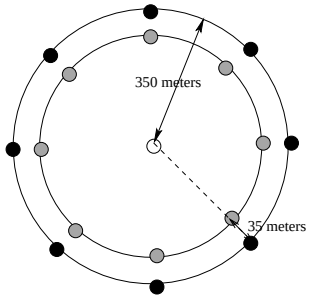

Fig. 8. Circular Topology with N = 8

Figure 9 presents the aggregate throughput for the topologies with N = 3, 8 and 32, respectively. In each plot, the payload packet size is 2048 bytes; x axis represents $\beta = \frac{CS_{th}}{RX_{th}}$ in dB (i.e., $10 \log \beta$) and is proportional to the value of the carrier sense threshold (CS_{th}); y axis represents the aggregate throughput in the unit of Mbps.

As we can observe from Figure 9(a), with only three transmitters in the network, the maximum throughput is achieved when operating at the highest data rate 54 Mbps with $\beta \geq -36dB$. Interestingly, when the total number of transmitters is increased to 8, the maximum throughput is obtained when the link data rate is set to 36 Mbps and $\beta \geq -22dB$, as shown in Figure 9(b). Further increasing the total number of transmitters to 32, the maximum throughput is then achieved when the link data rate is set to 18 Mbps and $\beta = -10dB$, which is illustrated in Figure 9(c).

Retransmissions lead to the bandwidth-dependent MAC overhead. Increasing the number of transmitters from 3 to 8 to 32, the channel contention increases. With 3 transmitters in the network, there is no retransmission occurring (i.e., no bandwidth-dependent overhead). When it goes to 32 transmitters, many retransmissions occur at each communication link, which leads to a significant amount of bandwidth-dependent overhead. The observations from Figure 9 agree with the analysis results we obtained in Section IV-C.2: the optimal carrier sense threshold increases (i.e., optimal carrier sense range decreases) when bandwidth-dependent overhead increases.

Now we examine each simulated topology more carefully. Using the topology with only three transmitters (Figure 9(a)) and choosing $\beta = -36dB$, all three

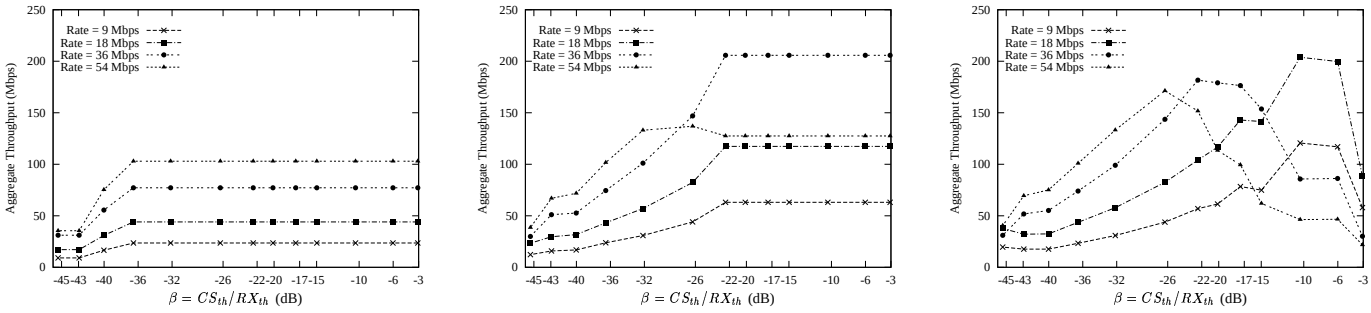

(a) N = 3 (b) N = 8 (c) N = 32

Fig. 9. Aggregate throughput vs. β (Packet Size: 2048 bytes)

transmitters can transmit concurrently and $SINR$ at each receiver meets the requirements for all data rates. Increasing β further does not change the performance since there are no more transmitters in the network. Hence, the curve remains flat for $\beta \geq -36dB$. With three concurrent transmissions, the throughput obtained by each transmitter/receiver pair is 34.3, 25.71, 14.67, 7.89 Mbps, corresponding to the link rate of 54, 36, 18, 9 Mbps, respectively. The channel utilization of each communication link is thus 0.635, 0.714, 0.815, 0.977, corresponding to the link rate of 54, 36, 18, 9 Mbps, respectively. As there is no retransmission occurring, the improved channel utilization at a lower link rate is mainly due to the reduced bandwidth-independent overhead. However, since the amount of spatial reuse is same for all data rates, and the improved channel utilization at the lower link rates is not enough to compensate for the reduction of the absolute link rate, in this particular topology, the maximum aggregate throughput is achieved when the communication operates at the highest rate 54 Mbps.

In the topology with eight transmitters (Figure 9(b)), the peak throughput using the data rate of 54 Mbps occurs at the point $\beta = -26dB$, where on average approximately four concurrent transmissions are allowed to meet the minimum $SINR$ requirement. On the other hand, using the data rates of 36, 18, 9 Mbps, all eight transmitters are allowed to transmit concurrently without interfering with each other when $\beta \geq -22dB$. Because of the improved channel utilization for each individual communication link, and the increased number of concurrent transmissions, the peak aggregate throughput using the link rate of 36 Mbps is 1.5 times that obtained using the link rate of 54 Mbps, even though the absolute link rate is lower (36 Mbps vs. 54 Mbps).

For the topology with 32 transmitters, the average number of concurrent transmissions and the amount of retransmissions experienced by each communication link are further illustrated in Figure 10. Figure 10(a) repeats the aggregate throughput presented in Figure 9(c), except that the peak throughput positions for link rates of 54, 36, 18 Mbps are marked as *Pos A* (link rate is 54 Mbps, $\beta = -26dB$), *Pos B* (link rate is 36 Mbps, $\beta = -22dB$) and *Pos C* (link rate is 18 Mbps, $\beta = -10dB$), respectively.

The average number of retransmissions (per second) normalized by the average number of concurrent transmissions is plotted in Figure 10(b). As we can see, at a lower link rate, not only the bandwidth-independent overhead is smaller (revealed by the better channel utilization we calculated for Figure 9(a) where there is no retransmissions), but also the bandwidth-dependent overhead associated with retransmissions is smaller. As we explained in Section IV-C.2, the corruption of the transmitted packet is mainly caused by two sources of interference. One is the concurrent transmissions from transmitters outside the carrier sense range. The other is the simultaneous transmission attempts from transmitters inside the carrier sense range. When using a smaller carrier sense range, the interference from concurrent transmitters outside the carrier sense range will increase, but the probability of being interfered by simultaneous transmitters inside the carrier sense range will decrease because of a smaller number of such stations.

By operating at a lower link rate, the increased interference from concurrent transmissions due to the use of a smaller carrier sense range is already priced in, since a lower link rate requires a lower $SINR$ threshold. Benefiting from the reduced probability of being interfered by simultaneous transmitters inside the carrier sense range, the number of retransmissions experienced at *Pos C* is much smaller than that at both *Pos B* and *Pos A*.

The average number of concurrent transmissions occurred is 5.3 at *Pos A*, 7.1 at *Pos B*, 14.6 at *Pos C*, as shown in Figure 10(c). We can see that increased

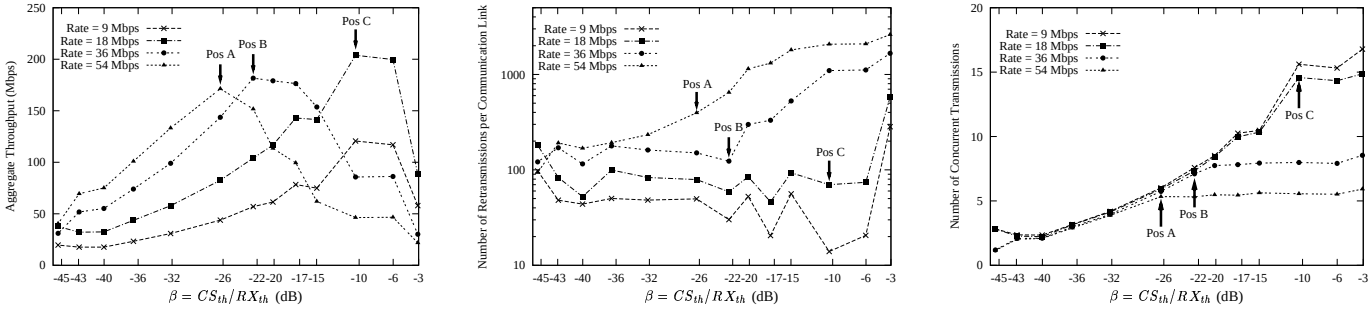

(a) Aggregate throughput (Mbps)

(b) The average number of retransmissions per communication link (per second)

(c) The average number of concurrent transmissions

Fig. 10. Elaboration on the topology with N = 32

carrier sense threshold largely increases the spatial reuse. Because of the improved spatial reuse, the reduced bandwidth-dependent and bandwidth-independent overhead at each communication link, the peak throughput achieved at *Pos C* is 1.14 times that at *Pos B* and 1.19 times that at *Pos C*, even though the absolute link rate at *Pos C* (18 Mbps) is only 1/2 of the link rate at *Pos B* (36 Mbps) and 1/3 of the link rate at *Pos A* (54 Mbps).

Similar simulations are performed for payload packet sizes of 512 bytes and 20 bytes. By reducing the payload size, the fraction of the link capacity wasted in bandwidth-independent overhead (due to physical preamble and header, interframe space and MAC layer backoff slots) increases. Figures 11(a) and 11(b) plot the aggregate throughput vs. β (in dB) for the topology of N = 32, with packet sizes of 512 bytes and 20 bytes, respectively (recall that Figure 10(a) plots similar results for packet size of 2048 bytes). Comparing the positions having peak throughput in Figures 10(a), 11(a) and 11(b), we can see a gradual trend of the optimal β and therefore, the optimal carrier sense threshold, increasing with the decrease of packet size (i.e., the increase of bandwidth-independent overhead). This observation is consistent with the analytical results in Section IV-C.1: the optimal carrier sense threshold increases (i.e., optimal carrier sense range decreases) when bandwidth-independent overhead increases.

The difference is more visible by comparing Figures 10(a) and 11(b). In Figure 11(b), the peak throughput for the link rate of 54 Mbps is achieved at $\beta = -22dB$ (marked as *Pos X* in the figure), compared with the peak point $\beta = -26dB$ in Figure 10(a) (*Pos A*); the peak throughput for the link rate of 36 Mbps is achieved at $\beta = -17dB$ (marked as *Pos Y*), compared with peak point $\beta = -22dB$ in Figure 10(a) (*Pos B*); the peak throughput for the link rate of 18 Mbps is achieved at $\beta = -6dB$ (marked as *Pos Z*), compared with the peak point $\beta = -10dB$ in Figure 10(a) (*Pos C*).

With the decrease of payload sizes, a greater throughput gap can also be observed among the peak points at different rates. In Figure 11(a), the throughput at *Pos F* is 1.25 times the throughput at *Pos E*, and 1.48 times the throughput at *Pos D*. In Figure 11(b), the throughput at *Pos Z* is 1.59 times the throughput at *Pos Y*, and 2.23 times the throughput at *Pos X*.

In summary, when applying a larger carrier sense threshold and operating at a lower link rate, the bandwidth-dependent and bandwidth-independent MAC overhead decreases and the channel utilization improves. As long as the source stations in the network can exploit the spatial reuse available in the network, we expect that the optimal carrier sense threshold that maximizes the aggregate throughput is larger (i.e., optimal carrier sense range is smaller), compared with the case in which the MAC overhead is not considered. As we mentioned in Section II, the existing research work does not consider the impact of MAC overhead when discussing the optimal carrier sense threshold, which can lead to a significant throughput loss.

VI. Conclusions and Future Work

The key observations in this paper are:

- MAC overhead has a significant impact on the choice of optimal carrier sense threshold. Applying a larger carrier sense threshold (i.e., a smaller carrier sense range) can lead to both the reduced bandwidth-independent MAC overhead and the reduced bandwidth-dependent MAC overhead, thus, improve the utilization of each individual wireless link. Even though the absolute throughput obtained

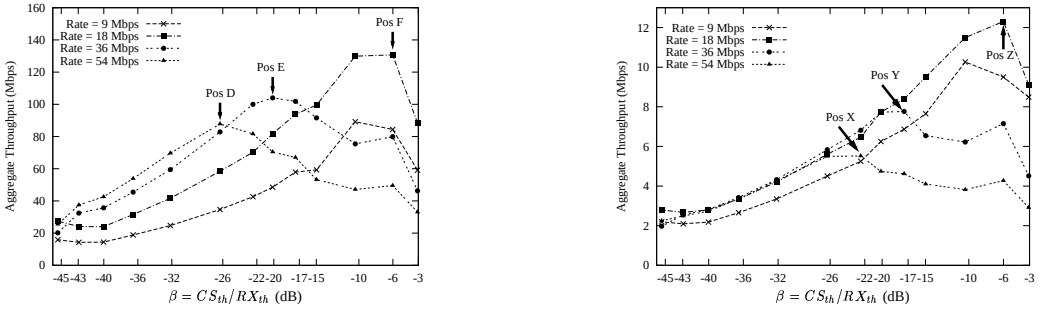

(a) Packet size: 512 bytes

(b) Packet size: 20 bytes

Fig. 11. Aggregate throughput vs. β (N =32)

by each transmitter/receiver pair may decrease because they operate at a lower link rate, the aggregate throughput can be improved as long as there are sufficient source stations to exploit the improved spatial reuse.

- The optimal carrier sense threshold depends on the degree of channel contention, packet size and other factors affecting the bandwidth-dependent and bandwidth-independent overheads. With an inappropriate choice of carrier sense threshold, the aggregate throughput can suffer a significant loss.

A dynamic spatial reuse and rate control algorithm can be motivated from our discussions to improve the aggregate throughput. Each station may adjust its carrier sense threshold based on current channel contention status (e.g., percentage of transmitted packets being corrupted), and data rate used by each communication link can be chosen based on the $SINR$ at the receiver.

To devise a distributed algorithm, each station needs to make its own decision based on the local channel status. However, as we mentioned before, whether aggregate throughput can be improved or not also depends on the amount of spatial reuse in the network. The amount of exploitable spatial reuse is closely related to the network topology, the radio propagation model, the communication rate between the transmitter/receiver pair as well as the carrier sense threshold applied to each station. While it is possible to deduce the utilization of each individual link based on local channel information, the amount of spatial reuse in the network concerns more global knowledge. How to make an effective local decision with regard to choosing proper values for carrier sense threshold and communication link rate without requiring too much global information imposes quite a challenge to the design of the algorithm. Another challenge is the stability of the algorithm. As seen from Figures 10(a), 11(a) and 11(b), an optimal combination of the carrier sense threshold and the communication link rate, which maximizes the aggregate throughput, is our desired operating point. However, wireless ad hoc networks are rich in turbulence. We need the optimal operating point to be stable such that the system, although perhaps fluctuating, tends to move in the direction of the optimal point. The exact definition and evaluation of such a dynamic spatial reuse and rate control algorithm is an ongoing activity.

REFERENCES

[1] Jing Zhu, Xingang Guo, L. Lily Yang, and W. Steven Conner, "Leveraging Spatial Reuse in 802.11 Mesh Networks with Enhanced Physical Carrier Sensing," in *IEEE International Conference on Communications (ICC'04)*, June 2004.

[2] P. Karn, "MACA - A new channel access method for packet radio," in *ARRL/CRRL Amateur Radio 9th Computer Networking Conference*, 1990, pp. 134–140.

[3] "Wireless LAN Medium Access Control (MAC) and Physical Layer (PHY) Specifications," June 1999, IEEE Standard 802.11.

[4] Kaixin Xu, Mario Gerla, and Sang Bae, "How effective is the IEEE 802.11 RTS/CTS handshake in ad hoc networks?," in *Proceeding of GLOBECOM'02*, 2002, vol. 1, pp. 72–76.

[5] Piyush Gupta and P. R. Kumar, "The capacity of wireless networks," *IEEE Transactions on Information Theory*, vol. 46, no. 2, pp. 388–404, March 2000.

[6] R. Hekmat and P. Van Mieghem , "Interference in Wireless Multi-hop Ad-hoc Networks and its Effect on Network Capacity," in *Med-hoc-Net*, September 2002.

[7] Xingang Guo, Sumit Roy, and W. Steven Conner, "Spatial Reuse in Wireless Ad-hoc Networks," in *VTC*, 2003.

[8] Gavin Holland, Nitin Vaidya, and Paramvir Bahl, "A rate-adaptive mac protocol for multi-hop wireless networks," in *ACM International Conference on Mobile Computing and Networking (MobiCom)*, July. 2001.

[9] B. Sadeghi, V. Kanodia, A. Sabharwal, and E. Knightly, "Opportunistic Media Access for Multirate Ad Hoc Networks," in *ACM International Conference on Mobile Computing and Networking (MobiCom)*, Sep. 2002.

[10] Zhifei Li, Sukumar Nandi, and Anil K. Gupta, "Improving MAC Performance in Wireless Ad Hoc Networks using Enhanced Carrier Sensing (ECS)," in *Third IFIP Networking Conference (Networking 2004)*, 2004.

[11] Sameh Gobriel and Rami Melhem and Daniel Mosse, "A Unified Interference/Collision Analysis for Power-Aware Adhoc Networks," in *Infocom*, March 2004.

[12] Marcelo M. Carvalho and J. J. Garcia-Luna-Aceves, "A Scalable Model for Channel Access Protocols in Multihop Ad Hoc Networks," in *ACM MobiCom*, Sep. 2004.

[13] T. D. Todd and J. W. Mark, "Capacity allocation in multiple access networks," *IEEE Trans. on Communications*, vol. COM-33, pp. 1224 – 1226, 1985.

[14] IEEE 80211b WG, "Part 11: Wireless LAN Medium Access Control(MAC) and Physical Layer(PHY) Specifications: Higher-Speed Physical Layer Extension in the 2.4 GHz Band," 1999, IEEE Standard 802.11.

[15] IEEE 80211a WG, "Part 11: Wireless LAN Medium Access Control(MAC) and Physical Layer(PHY) Specifications: High-speed Physical Layer in the 5 GHz Band," 1999, IEEE Standard 802.11.

[16] Marco Ajmone Marsan and D. Roffinella, "Multichannel local area network protocols," *IEEE Journal on Selected Areas in Communications*, vol. 1, no. 5, pp. 885–897, November 1983.

[17] J. Kivinen, X. Zhao, and P. Vainikainen, "Empirical characterization of wideband indoor radio channel at 5.3 ghz," *IEEE trans. on Antenna and Prop.*, vol. 49, 2001.

[18] Theodore S. Rappaport, *Wireless Communications: Principles and Practice (Second Edition)*, Upper Saddle River Prentice-Hall, 2002.

[19] W. C. Y. Lee, "Elements of Cellular Mobile Radio Systems," *IEEE Transactions on Vehicular Technology*, vol. VT-35, no. 2, pp. 48–56, May 1986.

[20] Matthias Grossglauser and David Tse, "Mobility increases the capacity of ad-hoc wireless networks," in *Infocom*, 2001.

[21] Bruce Hajek, Arvind Krishna, and Richard O. LaMaire, "On the capture probability for a large number of stations," *IEEE Trans. on Communications*, vol. 45, no. 2, pp. 254–260, 1997.

[22] John M. Wozencraft and Irwin Mark Jacobs, *Principles of Communication Engineering*, Prospect, IL: Waveland Press, Inc., 1990.

[23] F. Cali, M. Conti, and E. Gregori, "Dynamic tunning of the IEEE 802.11 protocol to achieve a theoretical throughput limit," *IEEE/ACM Trans. on Networking*, vol. 8, no. 6, pp. 785–799, December 2000.

[24] Jung Yee and Hossain Pezeshki-Esfahani, "Understanding wireless lan performance trade-offs," Nov. 2002, CommsDesign.Com.